JOURNAL OF COMPUTATIONAL PHYSICS 80, 387–402 (1989)

Linear Analysis of the Vortex-in-Cell Algorithm Applied to Rayleigh–Taylor Instability

JUAN A. ZUFIRIA

Applied Mathematics, California Insitute of Technology, Pasadena, California 91125

Received September 28, 1987; revised February 2, 1988

The effect of the grid in the vortex-in-cell algorithm on the linear growth rates for an interface undergoing Rayleigh–Taylor instability is studied. Results show that the effect of the grid is qualitatively equivalent to the effect of surface tension. It is also found that only wavelengths which are ten times longer than the grid spacing are resolved with error of less than 10% in the growth rate.

1. INTRODUCTION

Frequently in fluid mechanics we are interested in describing the evolution of a material line. Usually, this material line represents the interface between two fluids or two regions of the same fluid with different properties. In most of the cases the fluid line is highly unstable and the shape of the line becomes very complex. Typical examples of this are the Kelvin–Helmholtz and the Rayleigh–Taylor instabilities. In these two cases, when the fluid is assumed to be ideal, the interface is a vortex sheet whose vorticity is generated baroclinically.

During the last few years a great variety of numerical methods have been developed to study the evolution of these interfaces. Most of them represent the interface by a set of Lagrangian markers. Among these Lagrangian methods, we distinguish three of them, which are the boundary integral method, the point vortex method, and the vortex in cell (VIC) method.

In the boundary integral method [2] the evolution equations for the interface are written in terms of Fredholm integral equations. The resulting integral equations have convergent Neumann series and are solved by iteration. If M is the number of markers used to represent the interface, then the number of operations per iteration is of order M^2. This method has the problem that when the interface is highly deformed many markers are need to describe the interface and the iteration converges very slowly making the method computationally expensive.

In the point-vortex method [8] the vorticity of the interface is assumed to be concentrated in the markers and each marker is a point vortex with a given circulation. Here, the velocity of a marker is determined by a direct summation of the effect of all the point vortices on the marker. The summation is again of order

0021-9991/89 $3.00

M^2 operations. Again when the interface is complex M has to be large and the method becomes expensive.

Finally in the VIC metod [4, 7] the interface is again described by point vortices but instead of computing the velocity field on the markers by a direct summation, the Poisson equation for the stream function is solved on a given grid. The first step is to distribute the circulation of the markers on a fixed uniform grid (smoothing step). The Poisson equation for the stream function is solved on the grid for the vorticity distribution obtained from the smoothing step. And finally, the velocity at the interface is computed by some kind of interpolation from the results in the grid (interpolation step). This method has the advantage that the number of operations to compute the velocity at the interface are $O(N^2 \log(N))$, where N^2 is the number of grid points. But in general $N \ll M$, so the method is very cheap from the computational point of view.

As we have seen, the introduction of the grid produces a considerable reduction in the computational cost, but we have to pay some price for doing this. We are losing spatial accuracy in the results. The spatial resolution of the velocity field is of the order of the grid size. Baker's [1] work analyzing the rollup of vortex sheets shows that the large scale (relative to the grid size) motion is accurately reproduced by the VIC algorithm and the small scale motion is strongly affected by the grid. In the present work we try to give a quantitative estimate of the resolution that we lose by introducing the grid. We are going to focus our attention only on the spatial resolution and we will not deal with the errors associated to the time discretization of the evolution equations.

Moore [5] did the first analysis of the effect of the discretization on the accuracy of the point vortex method. He studied the accuracy of representing a vortex sheet by a set of point vortices. Here, we complement Moore's analysis by studying together the effect of the discretization of the vortex sheet into point vortices and the effect of the grid.

Our study will concentrate on the Rayleigh–Taylor instability. To measure the effectiveness of the method, in Section 2 we analytically obtain an expression for the linear growth rate of infinitesimal perturbations of different wavelengths on an initially flat interface which is Rayleigh–Taylor unstable. In Section 3 we compare these growth rates with the theoretical ones and give some conclusions.

2. Analysis of the Algorithm

Consider two superposed inviscid fluids which are initially separated by a straight horizontal interface in a gravity field. Let ρ_2 be the density of the upper fluid, and ρ_1 the density of the lower fluid. When $\rho_2 > \rho_1$ the interface is unstable. The interface behaves as a vortex sheet with strength $\gamma(s, t)$ which is determined by the evolution equation [7]

$$\frac{d\gamma}{dt} = 2A\left[\frac{d\mathbf{U}}{dt}\cdot\mathbf{s} + \frac{1}{8}\frac{\partial\gamma^2}{\partial s} + g\frac{\partial y}{\partial s}\right] - \gamma\frac{\partial\mathbf{U}}{\partial s}\cdot\mathbf{s}, \tag{1}$$

where the effect of the surface tension has not been considered. Here A is the Atwood ratio defined as

$$A = \frac{\rho_2 - \rho_1}{\rho_2 + \rho_1}. \tag{2}$$

$\mathbf{U}$ is the velocity at the interface defined as the average between the velocities in both sides

$$\mathbf{U} = \frac{\mathbf{u}_1 + \mathbf{u}_2}{2}. \tag{3}$$

The time derivative d/dt represents a total derivative following the interface and is related to the Eulerian derivatives by the expression

$$\frac{d}{dt} = \frac{\partial}{\partial t} + \mathbf{U} \cdot \nabla. \tag{4}$$

In Eq. (1), $\mathbf{s}$ is the unit vector tangent to the interface, s is the arclength, and g is the acceleration of the gravity. The interface is described by $\mathbf{x} = (x(s, t), y(s, t))$.

To describe the evolution of the vortex sheet, in addition to Eq. (1) we need the kinematic relations that describe the motion of the interface

$$\frac{d\mathbf{x}}{dt} = \mathbf{U}. \tag{5}$$

$\mathbf{U}$ can be computed in terms of the position $\mathbf{x}$ and the strength γ of the vortex sheet by solving the Poisson equation for the streamfunction.

To study the linear stages of the instability we linearize Eqs. (1) and (5). Taking into account that $\mathbf{u}_1 = \mathbf{u}_2$ on the interface in linear theory, the linear forms of Eqs. (1) and (5) is

$$\frac{\partial \gamma}{\partial t} = 2 \frac{\partial y}{\partial x}, \tag{6.1}$$

$$\frac{\partial y}{\partial t} = v, \tag{6.2}$$

where v is the vertical component of $\mathbf{U}$ and can be computed in terms of γ. Here all the variables have been made dimensionless taking as the basic length L, the width of the computational box, and as the basic time scale $\sqrt{L/Ag}$.

Equations (6) allow solutions of the form

$$\begin{aligned} \gamma &= \gamma^0 e^{\sigma t} e^{2\pi i k x}, \\ y &= y^0 e^{\sigma t} e^{2\pi i k x}. \end{aligned} \tag{7}$$

which describe the time evolution of infinitesimal perturbations of wave number k. σ represents the growth rate of the instability and is given by

$$\sigma = \sqrt{2\pi k}. \tag{8}$$

We are interested in studying the effect of the grid in the linear growth rate of the instability for a vortex-in-cell (VIC) simulation. To do this, we have to analyze the effect of each step of the VIC algorithm on an infinitesimal perturbation of a given wavelength k.

Let us assume that we have a grid which is periodic on the (0, 1) interval in the x direction and infinite in the y direction. Each cell of the grid is a square of side h, and $h = 1/N$. We will represent the vortex by Nm point markers, i.e., we assume m markers per cell (see Fig. 1). The VIC algorithm can be thought of as a linear operator which gives v as a function of γ, i.e,

$$v = L_{N,m}(\gamma). \tag{9}$$

The Fourier transform of the continuous version of this operator $\hat{L}$ is

$$\hat{L} = -i/2, \tag{10}$$

where $i = \sqrt{-1}$.

In the VIC algorithm we can distinguish three different steps. The first one is the distribution of the circulation of the markers on the grid (smoothing step). To perform this step we use the so-called area-weighting-rule (AWR) [4]. This step gives us a discrete distribution of vorticity $\omega_{j,n}$ on the grid, and the second step is to solve the Poisson equation for the streamfunction $\psi_{j,n}$ on the grid to determine the flow field. The boundary conditions that are assumed for the streamfunction are that ψ is periodic in x and goes to zero as $y \to \pm\infty$. In the third and last step, we

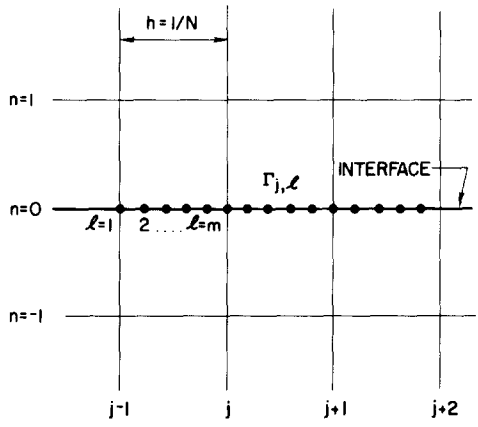

FIG. 1. Geometry of the problem.

interpolate the velocity field corresponding to the computed streamfunction for the interface again (interpolation). To perform this step two different methods are generally used. These methods are the AWR and the interpolation due to Peskin [6]. Both methods will be studied in the present work. We are going to analyze independently the effect of each of these three steps.

Before going into the analysis of the VIC algorithm, we analyze the spatial derivative of Eq. (6.1). Introducing (7) into (6.1) and using a centered difference scheme to compute the derivative along the arc length (notice s is equivalent to x in the linear analysis), we have that

$$\gamma = \frac{4\pi ik}{\sigma} y^0 e^{2\pi ikx} \alpha(a, m), \tag{11}$$

where $a = 2\pi kh$. The factor α is given by

$$\alpha(a, m) = \frac{m}{a} \sin\left(\frac{a}{m}\right). \tag{12}$$

This operation is independent of the grid. It depends only on the markers, i.e., $\alpha(a, m) = f(a/m)$. Notice that as $a/m \to 0$ then $\alpha \to 1$. In Fig. 2 we show α versus a for different values of m.

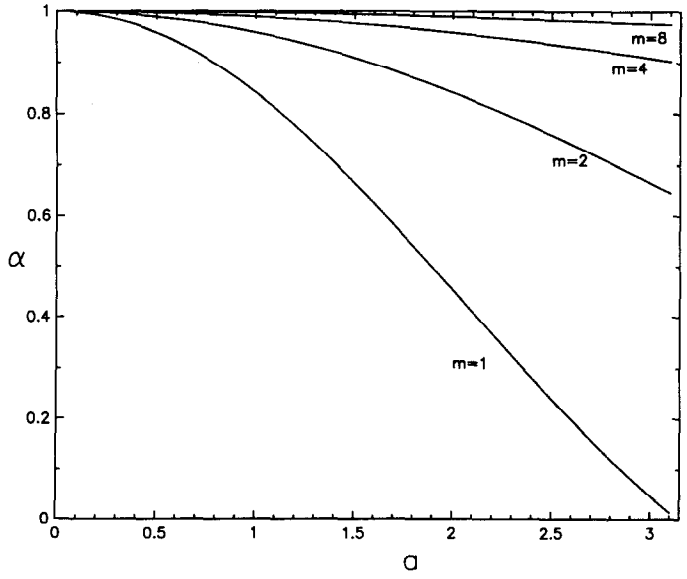

FIG. 2. Effect α of the spatial differentiation versus $a = 2\pi k/N$ for different values of m.

2.a. *Distribution of the Vorticity* (AWR)

The circulation associated with each of the markers Γ is defined as

$$\Gamma_{j,l} = \int_{e_-}^{e_+} \gamma(s, t)\, ds, \tag{13}$$

where e_- and e_+ represent mid points between markers (see Fig. 3).

Following the AWR the vorticity ω_j at the grid point j is given by (see Fig. 3)

$$\omega_j = \gamma^0 h e^{2\pi i k h(j-1)} \left\{ \frac{1}{m} + \frac{1}{m^2} \sum_{l=1}^{l=m} (m-l)[e^{2\pi i k h l/m} + e^{-2\pi i k h l/m}] \right\}. \tag{14}$$

To obtain this expression, the integral of Eq. (13) has been approximated by $\Gamma_{j,l} = \gamma_{j,l} h/m$ (see Figs. 1 and 3).

Performing the summation, Eq. (14) can be rewritten in the form

$$\omega_j = \gamma^0 h e^{2\pi i k(j-1)h} \beta(a, m), \tag{15}$$

where

$$\beta(a, m) = \frac{1}{m^2} \frac{1 - \cos(a)}{1 - \cos(a/m)}. \tag{16}$$

Notice that for fixed m, as $a \to 0$, $\beta \to 1$. Figure 4 shows β versus a for different values of m.

2.b. *Poisson Solver*

In this step we have to compute the flow field induced by the vortex sheet. This flow field satisfies the following Poisson equation

$$\Delta\psi = -\omega \tag{17}$$

on the grid.

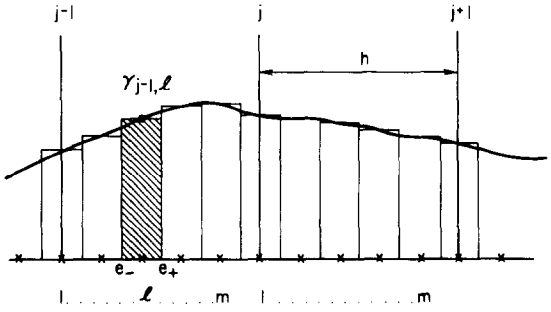

FIG. 3. Geometrical detail of the smoothing of the vorticity of the markers to the grid following the area-weighting-rule.

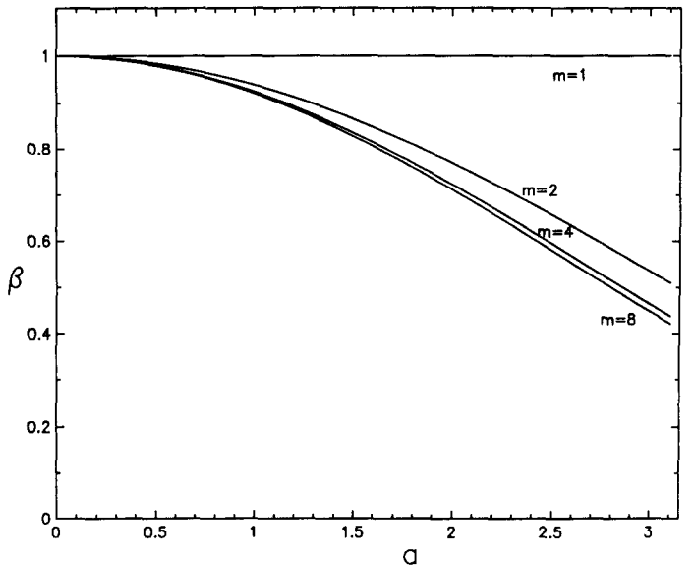

FIG. 4. Effect β of the smoothing step done by the area-weighting-rule versus $a = 2\pi k/N$ for different values of m.

To solve Eq. (17), we assume that the Laplacian operator has been discretized by using the standard five-point operator and we introduce the FFT in the periodic direction. The discrete Fourier transform $\hat{\omega}$ of the vorticity distribution ω_j contains only one mode $\hat{\omega}^{(k)}$. From (11) and (15) it follows that

$$\hat{\omega}^{(k)} = \frac{4\pi ik}{\sigma} \alpha\beta h y^0. \tag{18}$$

When the FFT is applied to the discretized Poisson equation we obtain a system of linear algebraic equations for each mode. Each of the equations comes from each row of the grid. In our case we have assumed that the grid extends up to infinity in the y direction, so that the system has an infinite number of equations. The form of these equations is

$$\hat{\psi}^{(k)}_{n+1} + 2\tau\hat{\psi}^{(k)}_n + \hat{\psi}^{(k)}_{n-1} = \begin{cases} 0 & \text{for } n \neq 0, \\ \omega^{(k)} & \text{for } n = 0. \end{cases} \tag{19}$$

where n indicates the row in the grid and goes from $-\infty$ to $+\infty$, and

$$\tau = \cos(a) - 2. \tag{20}$$

Thus we have to solve is a linear difference equation with given boundary conditions. The roots of the characteristic polynomial are

$$\begin{aligned} r_1 &= -\tau + \sqrt{\tau^2 - 1} \geqslant 1, \\ r_2 &= -\tau - \sqrt{\tau^2 - 1} \leqslant 1. \end{aligned} \tag{21}$$

As ψ has to vanish at $y = \pm\infty$, the solution of (19) can be written as

$$\hat{\psi}_n^{(k)} = \begin{cases} C_1 r_2^n & \text{for } n \geqslant 0 \\ C_2 r_1^{-n} & \text{for } n \leqslant 0. \end{cases} \tag{22}$$

To solve the system we have two additional conditions. The first one is that the solution has to be continuous at the interface ($n = 0$), and the second one is given by the difference equation at the interface. Satisfying these two conditions we obtain that $\hat{\psi}^{(k)}$ at the interface is given by

$$\hat{\psi}^{(k)} = -\hat{\omega}^{(k)} \frac{r_1}{2(1 + r\tau_1)}, \tag{23}$$

which can be rewritten as

$$\psi_j = \frac{1}{4\pi kh} \omega_j \delta(a), \tag{24}$$

where

$$\delta(a) = -\frac{ar_1}{1 + r\tau_1}. \tag{25}$$

Figure 5 shows δ versus a. Notice that δ is independent of the number of markers per cell m.

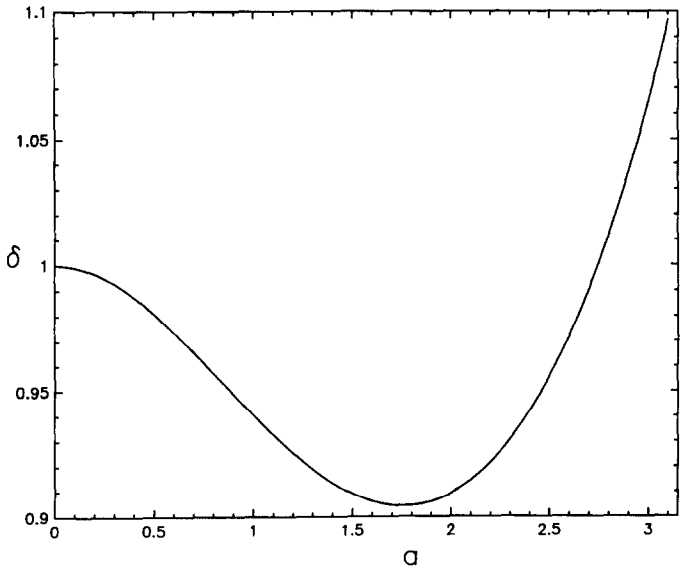

FIG. 5. Effect δ of the Poisson solver versus a.

This solution is valid only when $\tau \neq 1$. When $\tau = 1$ the solution does not vanish at $y = \pm\infty$. This occurs when $a = 0$ or $a = 2\pi$. Taking the limit as $a \to 0$ we find that $\delta \to 1$ and the solution is correct. When $a \to 2\pi$, $\delta \to 1/(2\pi - a)$. Notice that $a = 2\pi$ corresponds to $k = N$, i.e., the wavelength that we are considering is equal to the grid spacing.

2.c. *Velocity Field Interpolation*

We first consider the case in which the interpolation is performed by using the AWR. Assuming centered differences for the velocity, we have that the velocity at the interface within the interval $(j-1)h \leqslant x \leqslant jh$ is given by

$$-v(\xi) = \frac{\psi_{j+2} - \psi_j}{2h}\,\xi + \frac{\psi_{j+1} - \psi_{j-1}}{2h}\,(1-\xi). \tag{26}$$

If we evaluate (26) for the markers we have

$$v_{j,l} = \psi_j e^{2\pi i k(l-1)h/m}\left\{(e^{2a}-1)\frac{l-1}{m} + (e^{a}-e^{-a})\frac{m-l+1}{m}\right\}. \tag{27}$$

Finally, to relate y with v, we combine Eq. (6.2) with expressions (7) and (27). We multiply both terms of the equation by $\exp(-2\pi i k(l-1)h/m)$, and sum from $l = 1$ to $l = m$. After some algebra, we get

$$\sigma y_j = -2\pi i k \psi_j \zeta_A(a, m), \tag{28}$$

where

$$\zeta_A(a, m) = \frac{2\sin(a) - \sin(2a)}{2am^2[1 - \cos(a/m)]}. \tag{29}$$

Again we find that as $a \to 0$, $\zeta \to 1$. Figure 6 shows ζ versus a for different values of m.

As can be seen from Eq. (26), the AWR produces velocity distributions that are continuous but with a discontinuous derivative. Looking at Eq. (5), we can observe that the interface will also be continuous but with a discontinuous derivative. Looking for smoother velocity fields, another difference scheme has been sometimes used for this interpolation step. This scheme is due to Peskin [6]. The velocity at a point of the interface is defined in terms of the velocity at the grid points by the relation

$$v(x, y) = \sum_{j,n} v_{jn} h^2 D_{jn}(x, y), \tag{30}$$

where

$$D_{j,n} = d(x - [j-1]h)\, d(y - nh) \tag{31}$$

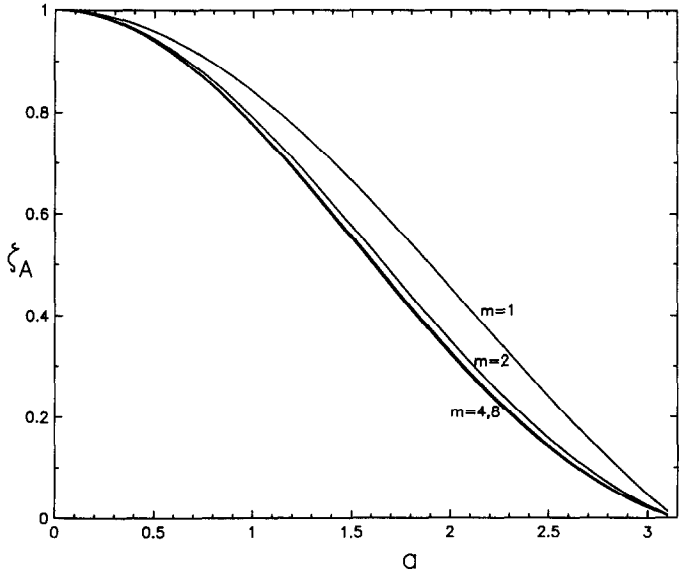

FIG. 6. Effect ζ_A of the interpolation step performed following the area-weighting-rule versus a for different values of m.

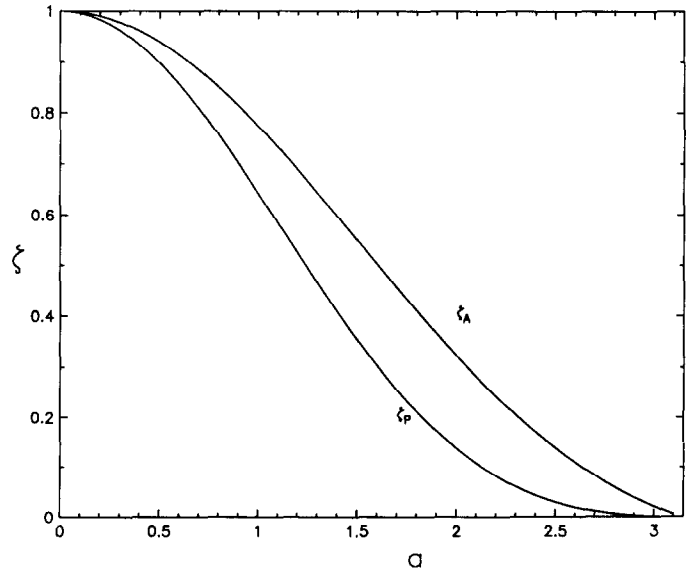

FIG. 7. Effect of the two different interpolating methods: ζ_A, area-weighting-rule ($m=8$); ζ_P, Peskin's interpolation.

and

$$d(r) = \begin{cases} (1/4h)(1+\cos(\pi r/2h)), & \text{for } |r| \leqslant 2h, \\ 0, & \text{for } |r| \geqslant 2h. \end{cases} \tag{32}$$

The weighting function $d(r)$ behaves in the grid as a discrete δ-function (see [6]).

A similar analysis can be done for this interpolation method, but the algebra becomes very messy in the case of finite m. However, in the limit of $m \to \infty$, the algebra is very simple and we find that

$$\zeta_P(a) = \frac{\cos(a) - \cos(3a)}{4a^2[1 - 4a^2/\pi^2]}. \tag{33}$$

In Fig. 7 we compare ζ_p and ζ_a. We can notice then even though Peskin's interpolation produces fields which are smoother than the ones produced by the AWR, this latter method is more accurate at reproducing the growth rate.

3. Results and Conclusions

In the previous section we have studied the effect of each one of the steps of the VIC algorithm on the growth rate of the linear instability. Here, we are going to consider the global effect. Using Eqs. (18), (24), and (28) we have

$$\sigma = \sqrt{2\pi k}\, \Theta_A(a, m), \tag{34}$$

where

$$\Theta_A^2(a, m) = \alpha\beta\delta\zeta_A. \tag{35}$$

Now we can observe that the linear operator associated to the VIC algorithm $\hat{L}_{N,m}$ defined in Eq. (9) is given by

$$\hat{L}_{N,m} = -\frac{i}{2}(\beta\delta\zeta)^{1/2}. \tag{36}$$

In Fig. 8 we show Θ_A versus a for different values of m. The first thing that we can notice is that the effect of m in Θ_A is very small and for $m \geqslant 2$ it can be assumed the Θ_A is independent of m. This means that the real effect of the discretization is due to the grid and not the number of markers. In Fig. 9 we again compare the two interpolation methods. Both methods have the same behavior, but the AWR gives better results. In the following we will consider only the AWR method.

To get a better idea of the meaning of Fig. 8, in Fig. 10 we compare the theoretical growth rate $\sqrt{2\pi k}$ with the growth rate obtained in the VIC for several values of N and for $m = 8$. We can notice that for k small the results are in very good agreement, but for large k the VIC does a poor job. The first thing that we

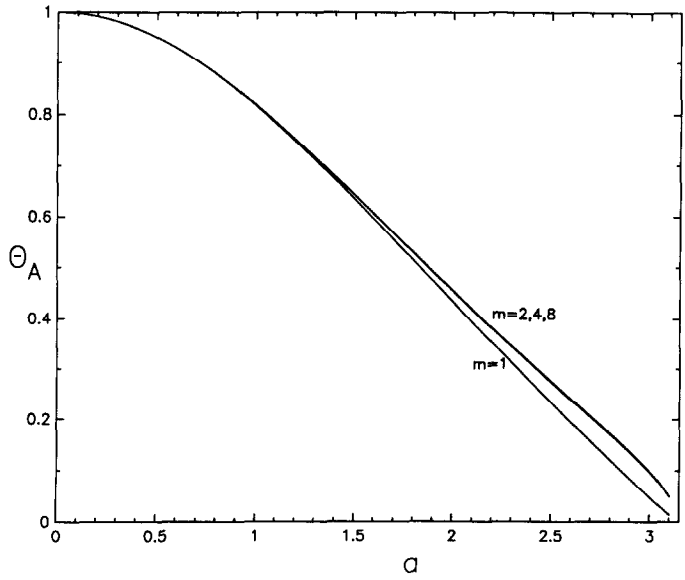

FIG. 8. Global effect Θ_A of the VIC algorithm using AWR in the interpolation step versus a for different values of m.

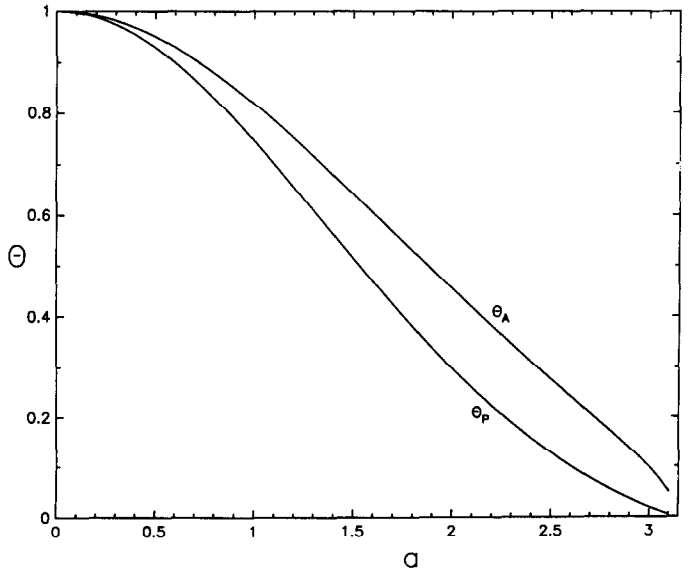

FIG. 9. Global effect Θ of the VIC algorithm using the two interpolating algorithms.

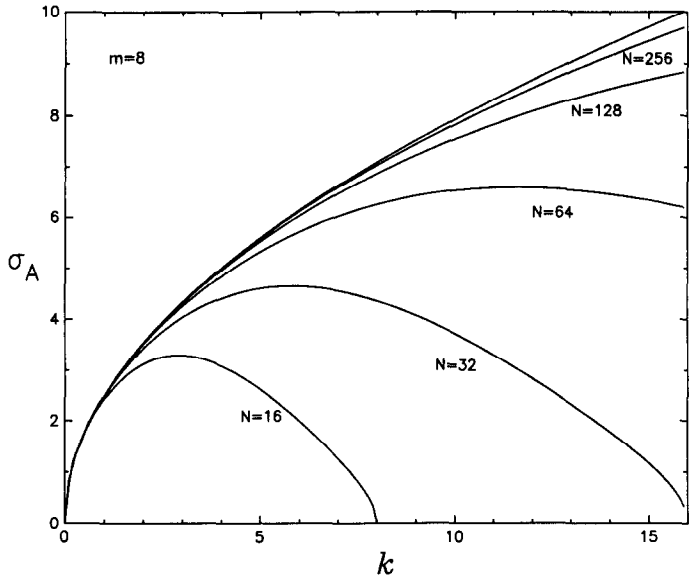

FIG. 10. Linear growth rate versus the wavenumber k for different grids. The top line represents the continuous results $\sigma = \sqrt{2\pi k}$.

notice is the appearance of a maximum growth rate. This maximum occurs at a wavenumber $k_{\max}$ which is approximately given by

$$k_{\max} \approx 0.180N. \tag{37}$$

Figures 11(a) and (b) show $k_{\max}$ and $\sigma_{\max} = \sigma(k_{\max})$ versus N.

Another important feature of the VIC growth rate is the existence of a wavenumber k^* for which the instability disappears; i.e., the interface is not unstable for all wavenumbers. Looking at Eqs. (29) and (35), it follows that this stabilization comes from the interpolation step. Notice that ζ_A becomes negative for $a > \pi$, i.e., $K > N/2$, whereas the others factors in (35) remain positive in the whole $(0, 2\pi)$ interval. Hence, we find that Θ_A is negative for $k > N/2$. This means that the modes $K > N/2$ do not grow and produce propagating waves.

All this behavior that we have found is similar to the behavior that is found in the continuous problem when surface tension is taken into account. With surface tension the linear growth rate is given by [3, p. 435]

$$\sigma^2 = 2\pi k(1 - Bk^2), \tag{38}$$

where

$$B = \frac{4\pi^2 T}{Ag(\rho_1 + \rho_2)L^2}. \tag{39}$$

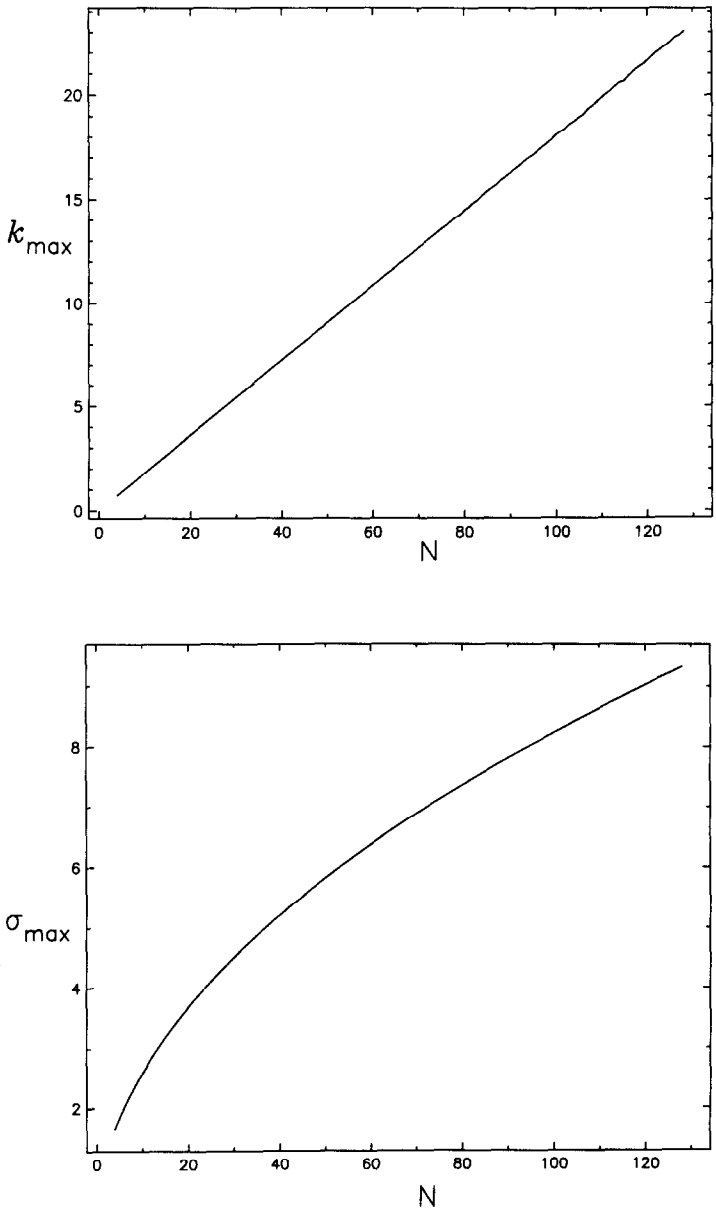

FIG. 11. (a) Wavenumber of maximum growth rate k_{max} versus the size of the gric. (b) Maximum growth rate σ_{max} versus the size of the grid.

T is the surface tension coefficient. The dimensionless parameter B is actually an inverse Bond number. The interface is unstable for wavenumbers in the range $0<k<k_c$, where $k_c=1/B^{1/2}$. For $k>k_c$ the disturbances propagate without growing. Unlike the case when surface tension is absent, there is a wavenumber $k_{\max}$ of maximum instability which is given by

$$k_{\max}=\left(\frac{1}{3B}\right)^{1/2}=\frac{k}{\sqrt{3}}. \tag{40}$$

The effect of the grid on the growth rate is qualitatively equivalent to the effect of the surface tension. In Fig. 12 we compare the growth rate for the VIC algorithm for $N=32$ and $m=8$ with the theoretical growth rate for $B=\frac{1}{256}$. Both curves have the same zeros and the same qualitative behavior. Hence, in some sense we could say that the effect of a grid of size $h=1/N$ is similar to adding a surface tension of $B=4/N^2$. This similarity with surface tension explains the rounded spikes found by Tryggvason [7] in computations with the VIC method for $A=1$, because surface tension tends to smooth out all the possible singularities on the interface.

From Fig. 9 it follows that to reproduce the growth rate of the instability with 10% accuracy with the AWR method, we need to have $a\leqslant 0.7$, i.e., $k/N\leqslant 0.111$. For a grid of $N=32$ only the three first wavenumbers are resolved with 10% accuracy. For the Peskin interpolation method we find that $k/N\leqslant 0.095$. This means that only wavenumbers which are ten times longer than the grid spacing h are resolved with an accuracy of 10%.

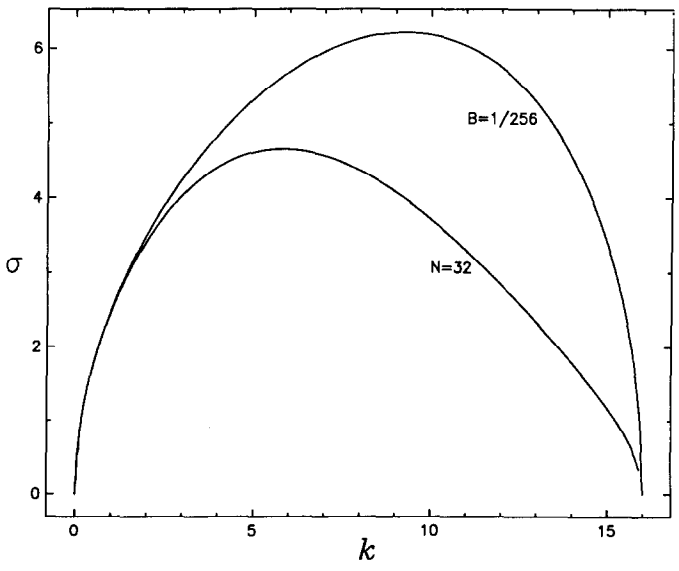

FIG. 12. Linear growth for $N=32$ in the VIC compared with the continuous growth rate for surface tension $B=\frac{1}{256}$.

Notice that the loss of accuracy comes essentially from the vorticity smoothing and velocity interpolation steps. The Poisson solver is quite accurate. This suggests that new distribution and interpolation schemes should be considered to improve the behavior of the vortex-in-cell method. The present analysis could be applied to higher order methods in an attempt to find better schemes.

ACKNOWLEDGMENTS

I want to thank Dr. M. Landman for suggesting this problem to me. I have also benefited from several discussions with Professors P. G. Saffman and D. I. Meiron. This work was supported by the Lawrence Livermore National Laboratory (7191705-DOEW-7405-ENG-48). I also wish to acknowledge an award from the Comité Conjunto Hispano-Norteamericano para la Cooperación Cultural y Educativa.

REFERENCES

1. G. R. BAKER, *J. Comput. Phys.* **31**, 76 (1979).
2. G. R. BAKER, D. I. MEIRON, AND S. ORSZAG, *J. Fluid Mech.* **123**, 477 (1982).
3. S. CHANDRASHEKHAR, *Hydrodynamic and Hydromagnetic Stability* (Oxford Univ. Press, Oxford, 1961), Chap. X.
4. J. P. CHRISTIANSEN, *J. Comput. Phys.* **13**, 363 (1973).
5. D. W. MOORE, in *Vortex Motion* edited by H. G. Hornung and E. A. Muller (Friedrich Vieweg, Braunschweig/Wiesbaden, 1982), p. 97.
6. C. S. PESKIN, *J. Comput. Phys.* **25**, 220 (1977).
7. G. TRYGGVASON, *J. Comput. Phys.*
8. S. J. ZAROODNY AND M. D. GREENBERG, *J. Comput. Phys.* **11**, 440 (1973).